This article has been accepted for publication in a future issue of this journal, but has not been fully edited. Content may change prior to final publication. Citation information: DOI 10.1109/TSG.2018.2794180, IEEE Transactions on Smart Grid

Adaptive Dynamic Simulations for Distribution Systems using Multi-State Load Models

K. P. Schneider, *Senior Member IEEE*, F. K. Tuffner, *Member IEEE*, M. A. Elizondo, *Senior Member IEEE*, J. Hansen, *Member IEEE*, J. C. Fuller, *Senior Member IEEE*, D. P. Chassin, *Senior Member, IEEE*,

***Abstract*— The deployment of new sensors and devices on electric distribution systems is increasing the awareness of phenomena characterized by intermittent periods of highly dynamic activity that occur within extended periods of relatively static behavior. The deployment of new devices has enabled the observation of these phenomena, however the currently available simulation methods cannot accurately reproduce the entire system behavior. Existing simulation methods, and their associated models, are able to capture portions of these phenomena, but there is not a method for efficiently modeling the entire event in a single simulation. This paper presents a novel method of adaptive simulation that enables automated transitions between quasi-static time-series (QSTS) and electromechancial simulation modes, as necessary to capture relevant system dynamics. The transitions between the simulation modes are triggered automatically during the running simulation based on the evolution of the system variables, utilizing multi-state modes for generators and motors. This method allows for a single simulation that spans the entire time-frame, has the ability to capture dynamic events, and includes all relevant power system controls. The method of adaptive simulation can support the direct analysis of dynamic power system events, co-simulation of transmission and distribution systems, the development of control systems, and the development of reduced-order models.**

***Index Terms*—Load modeling, power distribution, power system dynamics, power system simulation.**

NOMENCLATURE

$\delta(t)$	Generator rotor angle
$E_1(t)$	Generator internal positive sequence voltage
$E''_d(t)$	Generator subtransient voltage referenced to the *d*-axis
$E''_q(t)$	Generator subtransient voltage referenced to the *q*-axis
H	Generator inertial constant
$I_1(t)$	Generator positive sequence terminal current
$I_d(t)$	Generator *d*- axis current
$I_{INT}(t)$	Generator *dq*-referenced terminal current
$I_q(t)$	Generator *q*- axis current
$P_m(t)$	Generator mechanical power
$QSTS$	Quasi-static time-series
R_2	Generator negative sequence impedance
R_0	Generator zero sequence impedance
R_a	Generator armature resistance
R_S	Generator stator resistance
$S(t)$	Generator terminal apparent power
t	Time
$V_1(t)$	Generator positive sequence terminal voltage
V_d	Generator *d*-axis terminal voltage
V_q	Generator *q*-axis terminal voltage
$V_R(t)$	Generator *dq*-referenced terminal voltage
$V_T(t)$	Motor terminal voltage
$\omega_m(t)$	Mechanical (rotor) speed
ω_s	Synchronous speed
X_q	Generator armature reactance
Z_{Stall}	Motor stall impedance

I. INTRODUCTION

MODERN electrical power systems are highly dynamic systems with combinations of legacy infrastructure and new technologies [1]-[3]. As new technologies are deployed on the electric power systems, it is necessary to better understand the dynamics of the legacy infrastructure, including end-use loads [4]-[6]. In particular, it is necessary to simulate phenomena characterized by intermittent periods of highly dynamic activity that occur within extended intervals of more static system behavior. The commonly used 1-second or 1-minute nominal time-step, and the associated device and system models, of a quasi-static time-series (QSTS) simulation is able to run long duration simulations, hours to years, but it is not able to capture the higher frequency sub-

K. P. Schneider, F. K. Tuffner, M. A. Elizondo, and J. Hansen, are with the Pacific Northwest National Laboratory located in Seattle, WA 98109 USA. (e-mail: kevin.schneider@pnnl.gov, fransis.tuffner@pnnl.gov, marcelo.elizondo@pnnl.gov, jacob.hansen@pnnl.gov)

J. C. Fuller, is with the Pacific Northwest National Laboratory located in Richland, WA 99354 USA. (e-mail: Jason.fueller@pnnl.gov).

D. P. Chassin is with the SLAC National Accelerator Laboratory located in Menlo Park, CA 94025 USA. (e-mail: dchassin@slac.stanford.edu)

The Pacific Northwest National Laboratory is operated by Battelle for the U.S. Department of Energy under Contract DE-AC05-76RL01830. SLAC National Accelerator Laboratory is operated for the US Department of Energy by Stanford University under Contract DE-AC02-76-SF00515.

This article has been accepted for publication in a future issue of this journal, but has not been fully edited. Content may change prior to final publication. Citation information: DOI 10.1109/TSG.2018.2794180, IEEE Transactions on Smart Grid

second dynamics [7]. Sub-second dynamics can be examined with electromechanical and electromagnetic simulations, using millisecond and microsecond time-steps respectively [8]-[11]. However, existing commercial tools can typically only run electromechanical and electromagnetic simulations for approximately a minute [12]. The inability to run electromechancial simulations for more than approximately a minute is because of assumptions made in the models and controls. Specifically, the use of simplified load models and the omission of secondary and tertiary system controls; controls for devices such as tap changing voltage regulators and voltage controlled shunt capacitors at the distribution level are absent from most electromechancial simulations methods [13]. The absence of these controls can lead to inaccurate simulation results, and in many cases failures to converge.

One method for simulating events that occur over varying time scales is the use of variable time-steps; a method that can be used in QSTS, electromechanical, and electromagnetic simulations. Variable time-steps allow multi-month and annual QSTS simulations, but the underling models do not support dynamic simulation regardless of how small the time-step is [3], [9]. For the modeling of dynamic events, variable time-steps are commonly used in electromagnetic power electronic simulations in which the time-step is reduced during high-speed switching transients, and increased during periods of low-speed switching [12]. The use of variable time-steps for electromagnetic simulations works over relatively short time-periods, but is limited over extended time-periods. This limitation is due to numerical stability in the models and software, with electromagnetic time-steps over the 10 microsecond time-frame often causing divergence in the solution, and electromechanical time-steps over 100 milliseconds often causing divergence [14]

As a consequence of the solvers and models used, a purely QSTS simulation can run simulations over a long period of time such as hours to years, with large time steps such as 1-second to 1-hour, but cannot capture higher frequency dynamics, and electromechanical and electromagnetic simulation can capture higher frequency dynamics, but cannot be practically run over long periods of time. When a single simulation method cannot provide the desired capabilities, another option is to switch between simulation methods.

The IEEE Task Force on Interfacing Techniques for Simulation Tools conducted a literature review on methods for interfacing multiple tools in a single simulation environment [14]. The review of [14] examined the interfacing of electromagnetic transient simulations and transient stability simulations, the interfacing of circuit simulation programs with an electromagnetic field simulator, and the interfacing of real-time digital simulators. The work of [14] focused on simulations at the electromagnetic time-frame, so there was a limited ability to conduct simulations over extended periods of time.

A similar approach to individually interfacing tools is co-simulation, where multiple systems are simulated and the results federated in a single simulation environment [16]-[18]. Common systems that are federated under High Level Architecture (HLA)-type implementations include electric transmission systems, electric distribution systems, and communications systems [19]. Due to the different modeling representations used in these systems, it is common for each to use a different set of models and solvers, and their solutions matched at predefined boundaries. The co-simulator acts to coordinate the time sequencing and data exchange between the parallel simulations. Despite the advances in co-simulation technology, the individual parallel simulation are each run with a single model representation and set of solvers. The ability to adaptively switch a single simulation between solvers, within a running simulation, does not currently exist in any system-level power system simulation environment.

This paper presents a method of adaptively switching between two modes of simulation within a single running simulation environment: a QSTS mode using partial and ordinary differential equations (PDE/ODE) [20], and an electromechanical/phasor-dynamic mode using differential algebraic equations (DAE) [21], [22]. The adaptive simulation method allows the simulation to capture the higher frequency dynamics when they occur, and to transition to a faster QSTS representation during non-dynamic periods, allowing for extended simulation times that include secondary and tertiary controls to be included. The method of adaptively transitioning between simulation modes enables numerous transitions to occur without the need to re-initialize the entire simulation, enables the inclusion of secondary and tertiary controls, and reduces computation time while ensuring numerically stable. The method of adaptive simulation can support a range of analysis including determining distributed energy resource (DER) capacity analysis, planning studies for the integration of dynamic control devices, and impact studies for the deployment of dynamic end-use loads.

The effectiveness of the presented method is evaluated by examining the Fault-Induced, Delayed-Voltage Recovery (FIDVR) phenomena [23] on the IEEE 8500-Node Test Feeder [20], [24]. FIDVR is an example of a phenomena that can last for up to an hour, with only a small portion of that time containing higher frequency dynamics.

The rest of this paper is organized as follows: Section II presents the adaptive simulation method and Section III reviews the FIDVR phenomena. Section IV presents the model used for analysis, case studies, and simulation results. Section V contains the concluding comments.

II. Method of Adaptively Transitioning Between Simulation Modes

The use of variable time-steps in QSTS simulations allow for extended simulation periods, but they do not capture high frequency dynamics [7], [25]. Conversely, electromechanical simulations are able to capture high frequency dynamics, but typically produce inaccurate results, or numeric instability, when run over an extended period of time [13]. The combination of QSTS and electromechanical simulation modes, and the process to automatically transition between the two, provides a method to fully simulate the class of problems characterized by intermittent periods of highly dynamic activity that occur over an extended period of time.

The following sub-sections examine the differences between the QSTS and electromechanical simulation modes, how current co-simulation methods coordinate multiple simulation models, examples of the dynamic power system

This article has been accepted for publication in a future issue of this journal, but has not been fully edited. Content may change prior to final publication. Citation information: DOI 10.1109/TSG.2018.2794180, IEEE Transactions on Smart Grid

element models for each mode, and the process by which transitions between simulation modes are triggered.

A. QSTS vs. Electromechanical Simulations

QSTS simulations are a collection of steady-state power-flow solutions that may, or may not, have state variable information passed from one solution to the next. By passing state variable information, the simulations are more accurate, but this does not allow concurrent computation of steady state solutions [26]. The transition between time-steps is always assumed to be feasible since the system is transitioning from one steady-state solution to the next. As a result of the steady-state assumption, it is possible to increase the time-step between solutions with a minimal impact on numeric stability. The only exception to this is if there are load or control elements in the system that use an ODE/PDE representation with a time dependence. In this case, numeric stability can become a problem with larger time steps. Common time-steps for QSTS simulations are from 1 second to 1 minute [25], [26].

Electromechanical simulations are a series of power-flow solutions that are connected by propagating state variable information using DAEs, where the DAEs are initialized with a steady-state power-flow solution. The values of the state variables are then propagated forward in time, using the differential equations, by a defined time-step and then coupled through an algebraic power-flow solution [26]. Due to the non-linear time-dependent characteristic of power systems, numeric instability can occur if the time between algebraic solutions is allowed to be too large. The specific limits on the maximum time-step will depend on the analysis performed and the simulation package used, but common maximum values for electromechanical simulation are from 100 microseconds to 10 milliseconds [13].

B. Co-Simulation for Power Systems

Co-simulation is an active area of research where multiple systems are simulated concurrently and the results federated in a single simulation environment [16]-[19], [27]-[29]. The work presented in and [16], [19], and [27], presents co-simulation frameworks targeted towards electric transmission analysis with the inclusion of communications infrastructures. The authors in [18] and [29] provide additional fundamental research for co-simulating cyber-physical systems.

For the co-simulation approaches of [16], [19], and [27]-[29], it is common for each infrastructure to have a different set of solvers, and models, with their solutions matched at predefined model boundaries. In these applications, the co-simulation framework acts as the federator, ensuring that the individual simulators' boundary conditions are consistent over time. This approach offers flexibility in combining the output of various tools, but does not offer the ability for one simulator to change the underlying model or solver during simulation. While there are many software environments and hardware platforms that can perform simulations in multiple domains, there are no documented capabilities of being able to switch between QSTS and electromechanical simulations modes without stopping and restarting the simulation. Despite the inability of current co-simulation environments to be able to switch between simulation modes, one could be implemented in co-simulation. The next section presents a method that could be implemented in a stand-alone environment, or as part of a co-simulation platform.

C. Adaptive Transition between Simulation Modes

As discussed in the Introduction, it is not possible to use a single solver to simulate the class of electric power system problems characterized by intermittent periods of highly dynamic activity that occur over an extended period of time. This limitation exists whether using a stand-alone solver or a co-simulation framework. By adaptively switching between simulation modes this limitation can be addressed.

When transitioning between simulation modes, the equations used to represent the power system change between PDE/ODE and DAE. As a result, it is necessary to properly initialize the state variables of the equations when switching modes so that there are no significant discontinuities. If the initialization of state variables is not properly done during the transitions, discontinuities may appear resulting in artificial system transients and anomalous states. Additionally, if the discontinuities are large enough they have the potential to lead to instabilities in the simulation. The next two sections will provide examples of the process necessary to initialize state variables when transitioning between simulations modes, and the basis for determining when the transitions should occur.

D. Initializing State Variables during Simulation Mode Transitions

The following subsections review the QSTS and electromechanical dynamic representations of a synchronous generator using a subtransient model, and then discuss how the initialization of state variables is accomplished when transitioning between simulation modes. For these subsections, the model of a synchronous generator is examined [13], but the process is equally applicable to all dynamic elements that need to be initialized during transitions between simulation modes.

1) QSTS Representation of Synchronous Generator

In the power-flow solutions of the QSTS simulation mode, the synchronous generator is represented by a variable voltage swing/slack node with associated active and reactive power injections. If the generator is part of a microgrid, and there is no strong substation voltage source, it is assumed the generator has sufficient active and reactive power capabilities to maintain the system frequency and voltage. The internal, $E_1(t)$, and terminal voltages, $V_1(t)$, of the generator are related using (1), which translates to the synchronous generator apparent power output in (2).

$$E_1(t) = V_1(t) + \left(R_a + jX_q\right)I_1(t) \tag{1}$$

$$S(t) = V_1(t)\left(I_1(t)\right)^* \tag{2}$$

In (1) and (2) the 1-subscript denotes the positive sequence component of all values, and the asterisk operator represents the complex conjugate. Additionally, this simplified example only considers the positive sequence power values. For an unbalanced microgrid, a power-flow with synchronous machines can be handled via a shunt impedance and Norton-

This article has been accepted for publication in a future issue of this journal, but has not been fully edited. Content may change prior to final publication. Citation information: DOI 10.1109/TSG.2018.2794180, IEEE Transactions on Smart Grid

equivalent current source, and using machine characteristics, as explained in [21].

2) Electromechanical Representation of Synchronous Generator

In an electromechanical simulation, the differential equations of (3)-(5) represent the complete dynamic machine equations for a subtransient synchronous generator model [13].

$$\frac{2H}{\omega_s}\frac{d\omega_m(t)}{dt} = \frac{P_m}{\omega_m} - \left(E''_q I_q(t) - E''_d I_d(t)\right) - \left(R_2 - R_S\right) I_2^2(t) - D\left(\omega_m(t) - \omega_s\right) \quad (3)$$

$$\frac{dE''_d(t)}{dt} = \frac{\omega_m(t)}{\omega_s} E''_q + R_a I_q(t) + V_q(t) \quad (4)$$

$$\frac{dE''_q(t)}{dt} = \frac{\omega_m(t)}{\omega_s} E''_d + R_a I_d(t) + V_d(t) \quad (5)$$

From (3)-(5), it can be seen that the rotating machines use the commonly applied *dq*-axis representation [13]. Note that the *0*-axis is omitted in this model because the generator uses a balanced representation, however the use of a Norton equivalent can be used when the generator is connected to an imbalanced distribution system [21], [22]. The *dq*-axis representation is used to simplify analysis by transforming the model from a rotating to a fixed reference frame. The transformation from a rotating to a fixed reference frame yields constant-valued parameters for values such as inductance, rather than being rotor-position dependent [13].

Due to the different representations of the synchronous generator in QSTS and electromechanical modes, it is necessary to have a process to initialize the equations when transitioning between simulation models. This must be addressed during both the transitions from QSTS to dynamic mode and the transitions from dynamic mode back to QSTS. Failure to properly initialize the state variables may result in artificial transients in the dynamic simulation and anomalous states in the QSTS simulation.

3) Transition from QSTS to Electromechanical Simulations

During the transition from the QSTS to electromechanical mode, the complete set of state variables must be initialized to accurately represent the system conditions established by the previous QSTS power-flow solution. The state variables include the generator rotor angle, $\delta(t)$, the mechanical rotor speed, ω_m, and the direct and indirect subtransient voltages, $E''_d(t)$ and $E''_q(t)$. Since a power-flow solution is a steady-state condition, the machine speed and synchronous speed, ω_s, are assumed to be equal; the machine speed is initialized at the synchronous speed. In addition to the state variables, the mechanical and electrical power should also be equal so that there is no initial rotor angle acceleration.

Equations (6) - (10) show the relationship between the terminal voltage and current, and the internal state variables of the electromechanical dynamic representation. Equation (6) provides the initialization for the rotor angle, $\delta(t)$, of the synchronous model, based on (1).

$$\delta(t) = \angle E_1(t) \quad (6)$$

The initialized rotor angle from (6) is then used in (7) and (8) to apply the reference frame rotation to the machine. The rotation uses the *dq*-axis representation to obtain the *dq*-referenced terminal voltage and current, $I_{INT}(t)$ and $V_R(t)$, given the positive sequence representation [33].

$$I_{INT}(t) = jI_1(t)e^{j\delta(t)} \quad (7)$$

$$V_R(t) = je^{j\delta(t)}V_1(t) \quad (8)$$

Equations (9) and (10) relate the *dq*-referenced terminal voltage and current to the internal, subtransient voltages of the machine; both the direct, X'_d, and quadrature values, X'_q.

$$E''_d(t) = \mathrm{Re}\{V_R(t)\} + R_a \mathrm{Re}\{I_{INT}(t)\} - X'_q \,\mathrm{Im}\{I_{INT}(t)\} \quad (9)$$

$$E''_q(t) = \mathrm{Im}\{V_R(t)\} + R_a \,\mathrm{Im}\{I_{INT}(t)\} + X'_d \,\mathrm{Re}\{I_{INT}(t)\} \quad (10)$$

This section has shown how to initialize the state variables for a synchronous generator, but there are potentially additional state variables associated with the generator controls. For a diesel generator, these controls can include a speed control governor and an automatic voltage regulator (AVR). For a diesel generator using a subtransient synchronous generator model with speed control governor and AVR, there can be eleven or more variables to be initialized for a single generator [13]. This initialization must be done for every machine connected to the system, including inverter-connected generation. The process of initializing the state variable of the speed control governor, the AVR, and inverter-based generation follows the same process as the subtransient generator model shown in (6)-(10), but using the appropriate sets of equations [13].

4) Transition from Electromechanical Simulations to QSTS Mode

When a transition from dynamic to QSTS mode occurs, the initialization process is similar to the process presented in the previous section, but with important differences. Instead of initializing the state variables of the dynamic model, it is necessary to properly initialize the active and reactive power injections of the generator so that the steady-state powerflow solutions yields the same terminal voltage as the final value of the dynamic simulation.

The final result of (3)-(5), as well as the Norton equivalent implementation of [21], [22], provide the properly initialized current injection values for the subsequent QSTS simulation time-step. Coupled with the voltage solution from the algebraic power-flow equations and (1)-(2), these values result in the final power output of the generator and the new voltage setting for the swing/slack bus in the steady-state power-flow solution. Improperly initialized voltages may result in discontinuous reactive power-flows between the last electromechanical dynamic solution and the subsequent QSTS

This article has been accepted for publication in a future issue of this journal, but has not been fully edited. Content may change prior to final publication. Citation information: DOI 10.1109/TSG.2018.2794180, IEEE Transactions on Smart Grid

solution. Once the swing/slack bus voltage has been set, and any other buses where voltage is controlled by a generation source, the QSTS mode can proceed with the standard QSTS simulations.

E. Multi-State Load Modeling

The two previous sub-sections have detailed the process of properly initializing the state variables when transitioning between simulation modes. This section addresses how to determine when the transition should occur. For the use case examined in this paper, the FIDVR phenomena, the transitions are triggered based on the condition of the dynamics elements of the systems; specifically, the synchronous generators and the end-use induction motors.

Similar to the synchronous generator, the end-use load models require accurate representations in both the QSTS and electromechanical dynamic simulation modes. In the QSTS mode, the end-use motors are modeled using the traditional ZIP representations, which is a combination of constant impedance (Z), constant current (I), and constant power (P) elements [30]. The ZIP representation is a voltage depended load model that is appropriate for quasi-steady state simulations. In the electromechanical mode, the DAEs of [31] are used to represent the dynamic motor model. In both of the simulation modes the motor loads can transition between various operating states. To correctly model the various operational states of the motors it is necessary to use a multi-state load model [25]. An example state transition diagram for a single-phase motor is shown in Fig. 1.

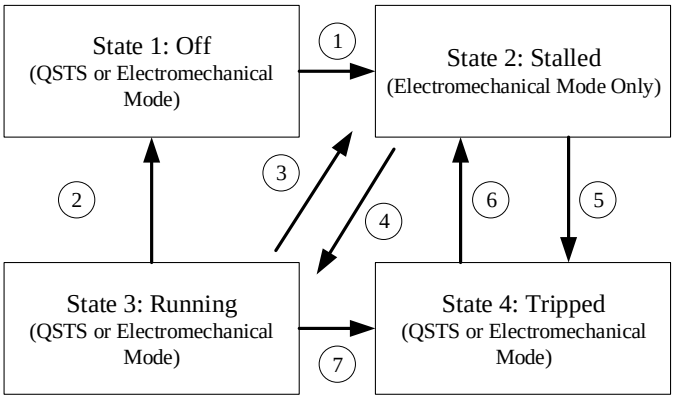

Fig. 1: State transition model for a single-phase induction motor, with allowed state transition paths shown as directional arrows.

For this work presented in this paper, a motor model with four operating states is used. The four states are shown in Fig. 1, with arrows indicating allowed transitions between states. This multi-state model is similar to the times-series models of [25]. Furthermore, the motor model will transition between QSTS and dynamic mode based on the grid conditions and rotor speed, to ensure that any high dynamic events are captured. Specifically, the motor model will monitor the terminal voltage, frequency, and rotor speed to determine if they fall below pre-defined constants. Table I gives the logic for the allowed state transitions shown in Fig. 1.

The allowed transitions shown in Fig. 1, and listed in Table I, are for a generic single-phase motor used for a heat pump, but there are variations between manufacturers. Using a generic set of transitions, as shown in Fig. 1, allows for simulations of the FIDVR phenomena. However, to exactly model a particular feeder, the model must be calibrated to operational field data. This is consistent with the usability of other end-use load models where calibration is required for a specific feeder [32]-[34].

TABLE I
STATE TRANSITION LOGIC FOR AN INDIVIDUAL INDUCTION MOTOR SHOWING THE LOGIC FOR ALLOWED TRANSITION PATHS SHOWN IN FIG. 1

Transition Path	From State	To State	Transition Rule
1	1	2	*motor manually started (initially stalled)*
2	2	1	*motor manually stopped*
3	3	2	ω_m <= *stall speed*
4	2	3	ω_m > *stall speed*
5	2	4	*thermal overload tripped*
6	4	2	*Thermal trip reset*
7	3	4	*thermal overload tripped*

Similar to the synchronous generator, the end-use motors are dynamic machines and their state variables must be initialized when transitioning between simulation modes. Unlike the synchronous generator, the end-use motors have multiple operating states which must be considered when initializing state variables. There are three scenarios where the state variables of the induction motor must be considered during state transitions. The first is when the simulation is running in QSTS mode and all the motor are about to stall, which automatically causes a transition to the electromechanical simulation mode; following transition path 3 in Fig. 1. A stalled motor in the electromechanical simulation mode is assumed to have no rotational speed and the power consumption in given by the locked rotor approximation as shown in (11).

$$S_{Motor} = \frac{\left(V_T(t)\right)^2}{Z_{Stall}} \tag{11}$$

When the single-phase motor stalls, there is an increase in power consumption as the impedance of the rotor decreases. The change in impedance, and the associated increase in power, can be calculated using the equations in [35].

Second, when a single motor stalls, following transition path 3 in Fig. 1, it is possible that other motors will continue to operate in the running state, State 3. Unlike the transitions to the stalled state discussed in the previous paragraph, the speed of the motors that continue to run will not drop to zero, but they may slow as a result of voltage reduction. Therefore, the state variables must be initialized between simulation modes to ensure an accurate continuous simulation. If the states are not properly initialized then there can be discontinuities led to inaccurate results for which motors stall and which are able to re-accelerate to their normal operating speed when the voltage is restored.

While the detailed process of initializing the state variables of a single-phase induction motor, outlined in [35], is not

This article has been accepted for publication in a future issue of this journal, but has not been fully edited. Content may change prior to final publication. Citation information: DOI 10.1109/TSG.2018.2794180, IEEE Transactions on Smart Grid

shown here, it follows the same process as shown in Section II-C for the synchronous generator. The third scenario is similar to the second, but occurs when tripped motors restart, following transition path 6, and the simulation transitions from QSTS to the electromechanical dynamic simulation mode. In this scenario, the motor uses an across-the-line controller so it must transition to the Stalled State, and then to the Running State once it is accelerated to its normal operating speed.

F. Basis for Transitioning Simulation Modes

The previous section discussed an isolated multi-state load model and how changes in its operational state can trigger a transition between operating models. Due to the fact that the simulation results for an entire distribution circuit are not known *a priori*, it is not known at which points in the simulation the transitions between simulation modes should occur. The transitions should occur based on the current conditions experienced by each of the dynamic elements, including their current operational state.

For the adaptive simulation method presented in this paper, the simulation remains in QSTS mode as long as there are no dynamic events. For a system with induction motors, the simulation remains in the QSTS mode as long as all motors are exhibiting normal grid conditions and the rotor speed is above its stall speed. If these conditions are not met for any motor, then the simulation enters the electromechanical dynamic mode. The simulation will remain in the electromechanical simulation mode until all motors have transitioned to the Running, Tripped, or Off State, the grid conditions have returned to normal, and the change in rotor angle, $\delta(t)$, for every generator, is less than 0.00001 rad/s between time-steps. The convergence criteria for the rotor angle can be adjusted depending on the specific analysis. A sufficiently small convergence criteria can force the simulation into the electromechanical mode for the entire simulation, and very large values can result in a failure to capture the system dynamics. A value of 0.00001 rad/s was empirically selected for this system when conducting a FIDVR analysis.

III. Fault-Induced Delayed Voltage Recovery

While there are many analyses that could benefit from the ability to adaptively transition between simulation modes, this paper uses the FIDVR phenomena as a use-case. The FIDVR phenomena is examined in limited detail so that the utility of the presented method can be evaluated; this paper will not address all aspects of FIDVR.

A. FIDVR Phenomena

The FIDVR phenomena is characterized by intermittent periods of highly dynamic activity that occur between intervals of quasi-static behavior. The dynamic behavior of a FIDVR event is driven by the dynamics of single-phase compressor motors, such as those commonly found in residential and commercial heat-pumps, air-conditioners, refrigerators, and freezers. These units are prone to stalling when their terminal voltage drops below approximately 80% of nominal for more than a couple of seconds [31]. It has been observed that three phase commercial motors are not as susceptible to stalling at lower voltages.

At low voltage levels, the electrical torque of the single-phase induction motor decreases below the mechanical torque and the rotor speed decreases to zero. The zero-speed response results in a locked rotor condition; referred to as a stall which is represented by State 2 in Fig. 1. When the rotor is stalled, the effective impedance of the rotor decreases, Z_{Stall} in (11). This impedance change results in a 4X-8X increase in the current drawn, which results in a 16X-64X increase in motor resistive heating; a combination of rotor and stator losses.

If the stalled conditions persist, the motor's thermal protection elements will eventually trip, typically between a few seconds and up to 30 seconds [36]. As the induction motors begin to trip off-line, the active and reactive load on the system is reduced and there is a corresponding recovery of the system voltage. After the initial stages of the FIDVR event, <100 seconds, the motors will begin to restart as their thermal masses cool, resulting in the thermal overloads resetting. The restarting of motors results in intermittent dynamic events as individual motors restart, occurring over a period of tens of minutes depending on external air temperatures.

Numerous FIDVR events have been reported in various regions of the United States, including Southern California, Florida, and Georgia [23], [37], and studied using electromagnetic transient program (EMTP) simulations [38]. The stages of the FIDVR phenomena have been well-documented and are shown in Fig. 2.

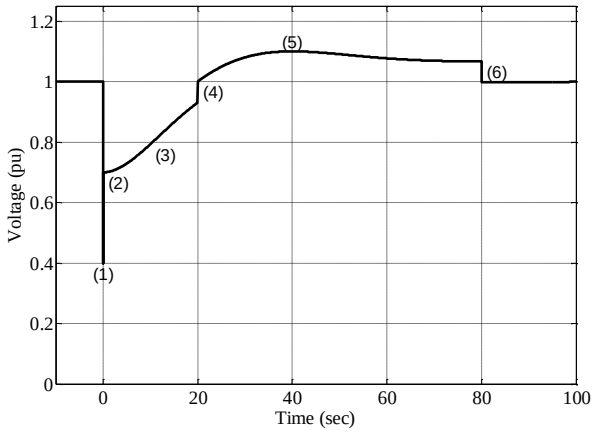

Fig. 2: Typical FIDVR event: initial fault (1), voltage recovery and motor stall (2), thermal tripping (3), voltage control up (4), voltage overshoot (5), voltage control down (6).

B. Current Method of FIDVR Modeling

FIDVR is primarily attributed to the dynamic behavior of single-phase motors in response to a transmission-level fault, and the subsequent interaction of voltage control devices; these voltage devices are secondary and tertiary control systems. A significant amount of past work on FIDVR has focused on improving the dynamic electromechanical end-use load models, which are the source of the high frequency dynamics. This work led the North American Electric Reliability Corporation (NERC) to provide guidance on load modeling in the early 1990s [32], [33]. In 2002, the Western Electric Coordinating Council (WECC) adopted an "interim" load model to address critical operating issues over the

This article has been accepted for publication in a future issue of this journal, but has not been fully edited. Content may change prior to final publication. Citation information: DOI 10.1109/TSG.2018.2794180, IEEE Transactions on Smart Grid

California-Oregon Intertie [39], and tasked the WECC Load Modeling Task Force (LMTF) to develop a composite load model to support dynamic planning and operating studies [40], [41].

More recent studies of FIDVR showed the effectiveness of detailed loads models under asymmetric fault condition, and the work in [42] presented a multi-port three-phase Thévenin equivalent to represent an external network in an electromagnetic transient simulator. Recent sensitivity analysis of the composite load model, using the PSLF® and PSS/E® commercial simulation packages, has provided an indication of which load characteristics are most relevant to FIDVR behavior [42], [43].

Much of the past work on FIDVR focused on the development of reduced-order dynamic load models for use in transmission-level simulations that could be used for an electromechanical simulation with a fixed time-step over a short period of time. There has not been any significant work to simulate an entire FIDVR event in a single model.

IV. Simulation Example

In this section, a 30-minute simulation of a FIDVR event is conducted on a modified version of the IEEE 8500-Node Test Feeder [20], [24], [44]. Two specific cases are examined. In Case 1, the results from a 30-minute simulation of the modified 8500-Node Test Feeder are presented, where the electromechanical dynamic simulation is run with a fixed 200 microsecond time-step. In this case, there is a voltage drop that causes motor stalling, and tripping of all of the induction motors on the system. The simulation is run for 30 minutes to capture both the initial system response, the system response as the thermal overloads of the motors reset, and the voltage restoration after the motor have restarted. Case 2 runs the same scenario as Case 1, but the simulation is allowed to transition between QSTS and electromechanical mode; when in electromechancial mode the same fixed 200 microsecond time-step is used as in Case 1.

The simulations for both cases in this section are run using the GridLAB-D™ open-source simulation environment [45]. GridLAB-D™ was selected because of its ability to implement controls at the device and system level, and because of its ability to implement multi-state load models in both QSTS and electromechanical simulation modes [25].

A. System Model used for Simulations

The 8500-Node Test System has been selected because the PES Test Feeder Working Group has not yet completed a formal microgrid model [44]. Additionally, this model is an accurate representation of the size and complexity of distribution circuits that are commonly deployed in North America, and specifically within the WECC where a large amount of FIDVR work has been conducted.

Two primary modification to the 8500-Node Test Feeder have been made for this work. The first modification is the replacement of a portion of the static load with 420 single-phase dynamic motor models at the end of the secondary triplex lines [30]; each motor is ≤ 3.0 horsepower. The second modification is the inclusion of detailed end-use load models that make use of Typical Meteorological Year (TMY) data so that weather conditions are properly represented [46]. The inclusion of detailed motor models and weather data are what allow the modified version of the 8500-Node Test System to be an effective model for FIDVR analysis.

B. Case 1: Fully Electromechanical Simulation

In Case 1, a completely electromechanical simulation with a fixed time-step of 200 microseconds is conducted; there are no transitions to a QSTS mode. This case was carefully selected to avoid the potential convergence issues that electromechancial simulations can experience when run for tens of minutes. Specifically, a relatively short duration reduction in voltage and the use of detailed voltage dependent end-use load models were implemented. The voltage regulators and shunt capacitors we not allowed to operate since the simulation remained in the electromechanical mode the entire time; consistent with many commercial packages.

In Case 1, the primary distribution voltage at the substation initially starts at approximately 7,300 V, line-to-neutral, and then there is a transmission-level fault at t=5.0 seconds, which reduces the substation voltage to approximately 5,000 V. The low voltage condition causes the induction motors to stall, transitioning from State 3 to State 2, following transition path 3 in Fig. 1, which increases the system load. The increased load results in a persistent low voltage, even when the fault is cleared. As a result of the persistent low voltage, the majority of single-phase motor overloads trip, transitioning to motors State 4, following transition path 5, within approximately four seconds of the transmission level fault (by t=8.5 seconds). It should be noted that there are four motors that are still in the stalled condition when the voltage is restored, at which point they accelerate back to normal operating speed, following transition path 4. As a result, after t=8.5 seconds there are 4 motors in State 3, and 416 motors in State 4. The operational states for the population of single-phase motors for the first 9.0 seconds of the FIDVR simulation are shown in Fig. 3.

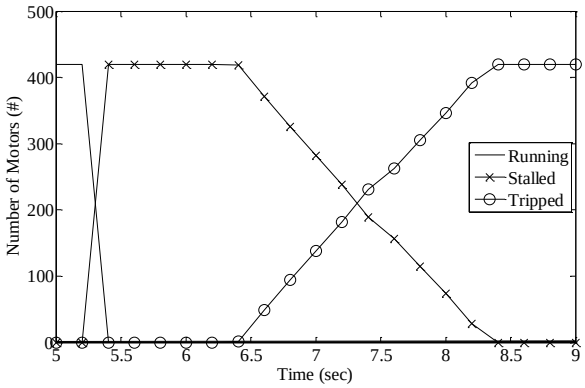

Fig. 3: Motor states during the initial voltage drop and subsequent voltage overshoot shown in Fig. 2. The population of motors is initially in the Running State, they then transitions to the Stalled State, and then the majority of motors transition to the Tripped State when their thermal overloads trip.

After the thermal overloads have tripped, the motors will not restart until the overloads have cooled. The thermal cooling period can take several minutes. For this simulation, TMY2 data is used to represent a warm day, which results in longer cool down times. The time for individual units to cool down is a uniform distribution of between 300 seconds and 1,800 seconds [47].

This article has been accepted for publication in a future issue of this journal, but has not been fully edited. Content may change prior to final publication. Citation information: DOI 10.1109/TSG.2018.2794180, IEEE Transactions on Smart Grid

In Fig. 4, it can be seen that the motors begin to transition from the Tripped State to the Stalled State, following transition path 6, and then to the Running State, following transition path 4, at between 300 seconds and 1,800 seconds. During this time, motors are continually starting, causing small dynamic disturbances on the system. For Case 1, the simulation remains in the electromechanical mode regardless of the operational states of the single-phase motors.

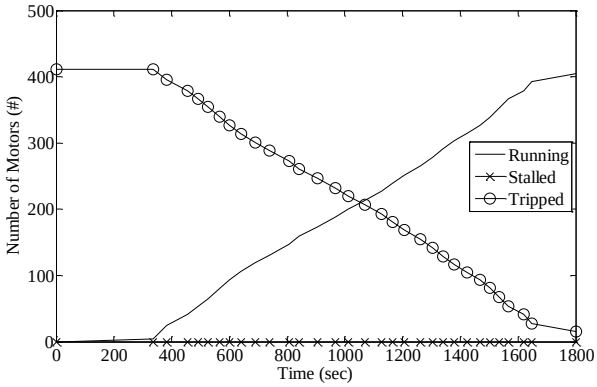

Fig. 4: Motor states during the entire simulation, with the traces of Fig. 3 compressed on the left hand y-axis. After 9.0 seconds the majority of motors are in the Stalled State and remain so until they begin to cool down. At approximately 300 seconds the overloads on individual motors begin to reset casing a transition to the Stalled State and then to the Running State.

The simulation results shown in Fig. 3 and Fig. 4 were obtained by running the modified version of the 8500-Node Test Feeder in an electromechanical dynamic simulation with a fixed time-step of 200 microseconds, for a one-hour simulation period. The total simulation time was 661.6 hours running on an Intel i7-6920HQ CPU@ 2.90 GHz with 16GB of RAM.

C. Case 2: Electromechancial Dynamic Simulations with Transitions

In Case 2, the simulation starts in QSTS mode and first transitions to the electromechanical dynamic mode when there is a voltage drop that results in motors decelerating prior to stalling. The simulation then stays in the dynamic mode until all of the motors have tripped at approximately t=8.4 sec. and then transitions back to QSTS mode. The simulation stays in QSTS mode until the motors begin to restart at approximately 300 sec. and transitions numerous times between QSTS and electromechanical dynamic mode as each of the motors restarts.

The voltage at individual nodes for Case 2 are similar to the results of Case 1. The difference in simulation results is <0.1% in average voltage magnitude at each node. It should be noted that in Case 1 the voltage regulators did not operate because the simulation was continually in electromechancial mode. As a result, there were no changes in regulator tap positions. This is consistent with the fact that the majority of commercial tools exclude many secondary and tertiary distribution voltage control during dynamic simulations. In Case 2 there were numerous voltage regulator tap changes. As a result, the simulation more accurately capture the behavior of the system during the FIDVR event.

Another significant difference is that in Case 2 the simulation transitions between QSTS and electromechanical dynamic mode numerous times. There are over 400 transitions between QSTS and the dynamic mode. Even with the large number of transitions, the simulation time was reduced to 2,322 minutes from 39,696 minutes, a factor of 17X speed up. This shows that even with the computational overhead associated with initializing the state variables at each of the numerous transition, the adaptive method of simulation is significantly faster than a purely dynamic simulation, while maintaining numeric stability and better representing the response of system controls during the FIDVR event.

V. CONCLUSIONS

The ability to conduct simulations that can adaptively transition between QSTS and dynamic modes provides a significant increase in analysis capability for distribution and microgrid simulations. This paper has presented a numerically stable method of adaptive QSTS/electromechancial simulation that enables the simulation of phenomena characterized by intermittent periods of highly dynamic activity that occur within extended interval of quasi-static behavior. The method presented shows how to properly initialize the state variables at each transition so that numerous transitions can occur without introducing anomalous transients, and how to model end-use loads to determine when the transition between simulation modes should occur.

The method of adaptive simulation was examined with the FIDVR example using the GridLAB-D™ simulation environment, however the method can be applied to a wide range of analysis and can be conducted with other simulation environments. Future work will examine the use of the adaptive simulation method to develop control algorithms for resiliency based microgrid operations, to evaluate the dynamics of transactive control systems, and to validate reduced order load models for co-simulation environments.

VI. REFERENCES

[1] "American Recovery and Reinvestment Act (ARRA) of 2009," June 2010, available: https://energy.gov/oe/information-center/recovery-act [Accessed: December-2017]

[2] D. J. Hammerstrom, D. Johnson, C. Kirkeby, Y. P. Agalgaonkar, S. T. Elbert, O. A. Kuchar, M. C. Marinovici, R. B. Melton, K. Subbarao, Z. T. Taylor, B. Scherer, S. Rowbotham, T. Kain, T. Rayome-Kelly, R. Schneider, R. F. Ambrosio, J. Hosking, S. Ghosh, M. Yao, R. Knori, J Warren, J. Pusich-Lester, K. Whitener, L. Beckett, C. Mills, R. bass, M. Osborne, and W. Lei, "2015 Pacific Northwest Smart Grid Demonstration Project Technology Performance Report Volume 1: Technology Performance," PNWD-4445, vol. 1, Battelle-Pacific Northwest Division, Richland, WA.

[3] K. P. Schneider, F. K. Tuffner, M. A. Elizondo, C. C. Liu, Y. Xu, and D. Ton, "Evaluating the Feasibility to use Microgrids as a Resiliency Resource," *IEEE Trans. on Smart Grid*, vol. 8, no. 2, pp 687-696, Mar. 2017.

[4] B. Palmintier, B. Lundstom, S. Chakraborty, T. Williams, K. Schneider, and D. Chassin, "A Power-Hardware-in-the-Loop Platform with Remote Distribution Circuit Co-Simulation," *IEEE Trans. on Industrial Electronics*, vol. 62, no. 4, pp 2236-2245, Nov. 2014.

[5] J. C. Fuller, S. Ciraci, J. A. Daily, A. R. Fisher, and M. L. Hauer, "Communications Simulations for Power System Applications," in *proc. IEEE Workshop on Modeling and Simulation of Cyber-Physical Energy Systems (MSCPES)*, 2013.

[6] Y. Cao, X. Shi, Y. Li, Y. Tan, M. Shahidehpour, and S. Shi, "A Simplified Co-Simulation Model to Investigate Impacts of Cyber-

Contingency on Power Systems," *IEEE Transaction on Smart Grid*, vol. PP, no. 99, 2017.

[7] R. Hunsberger and B. Mather, "Temporal Decomposition of Distribution System Quasi-Static Time-Series Simulations," in *proc. IEEE PES General Meeting*, 2017.

[8] K. Yu, Q. Ai, S. Wang, J. Ni, and T. Lv, "Analysis and Optimization of Droop Controller for Microgrid System Based on Small-Signal Dynamic Model," *IEEE Trans. on Smart Grid*, vol. 7, no. 2, pp. 695-705, Nov. 2016.

[9] K. P. Schneider, F. K. Tuffner, M. A. Elizondo, C. C. Liu, Y. Xu, S. Backhaus, and D. Ton, "Enabling Resiliency Operations across Multiple Microgrids with Grid Friendly Appliance Controllers," *IEEE Trans. on Smart Grid*, vol. PP, no. 99, pp. 1-1, 2017.

[10] D. Montenegro, G. Raos, and S. Bacha, "Multilevel A-Diakoptics for the Dynamic Power-Flow Simulation of Hybrid Power Distribution Systems," *IEEE Trans. on Industrial Electronics*, vol. 12, no. 1, pp. 267-276, Dec. 2016.

[11] J. C. G. de Siqueira, B. D. Bonatto, J. R. Jorge, J. A. Hollman, and H. W. Dommel, "Optimum Time Step Size and Maximum Simulation Time in EMTP-based Programs," in *proc. Power System Computation Conference*, 2014.

[12] M. B. Patil, V. Ramanaratanan, and V. T. Ranganathan, "Simulation of Power Electronic Circuits," Alpha Science International, Ltd., 2009.

[13] P. Kundur, "Power System Stability and Control," McGraw-Hill, 1994.

[14] M. Stubbe, A. Bihain, J. Deuse and J. C. Baader, "STAG-a New Unified Software Program for the Study of the Dynamic Behavior of Electrical Power Systems," *IEEE Trans. on Power Systems*, vol. 4, no. 1, pp. 129-138, Feb. 1989.

[15] V. Dinavahi, M. Steurer, K. Strunz, and J. A. Martinez, "Interfacing Techniques for Simulation Tools," in *Proc. IEEE PES General Meeting*, 2009.

[16] W. Li, M. Ferdowsi, M. Stevic, A. Monti, and F. Ponci, "Cosimulation for Smart Grid Communications," *IEEE Trans. on Industrial Informatics*, vol. 10, no. 4, pp. 2374 - 2384, July 2014.

[17] J. C. Fuller, S. Ciraci, J. A. Daily, A. R. Fisher, and M. L. Hauer, "Communication Simulations for Power System Applications," in *proc. IEEE Workshop on Modeling and Simulation of Cyber-Physical Energy Systems (MSCPES*), 2013.

[18] A. T. Al-Hammouri, "A Comprehensive Cosimulation Platform for Cyber-Physical Systems," *Computer Communications*, vol. 36, no. 1, pp. 8-19, Dec. 2012.

[19] J. C. Fuller, S. Ciraci, J. A. Daily, A. R. Fisher, and M. Hauer, "Communication Simulations for Power System Applications," in *proc. Modeling and Simulation of Cyber-Physical Systems*, 2013.

[20] K. P. Schneider and J. Fuller, "Voltage Control Devices on the IEEE 8500 Node Test Feeder," in *proc. IEEE PES T&D Conference and Exposition*, 2010.

[21] M. A. Elizondo, F. K. Tuffner, and K. P. Schneider, "Simulation of Inrush Dynamics for Unbalanced Distribution Systems using Dynamic Phasor Models," *IEEE Trans. on Power Systems*, vol. 32, no. 1, pp. 633-642, April 2017.

[22] M. A. Elizondo, F. K. Tuffner, K. P. Schneider, "Three-phase Unbalanced Transient Dynamics and Power-flow for Modeling Microgrids with Synchronous Machines," *IEEE Trans. on Power Systems*, vol. 31, no. 1, pp. 105-115, Jan. 2015.

[23] B. R. Williams, W. R. Schmus and D. C. Dawson, "Transmission Voltage Recovery Delayed by Stalled Air Conditioner Compressors," *IEEE Trans. on Power Systems*, vol. 7, no. 3, pp. 1173-1181, Aug. 1992.

[24] R. F. Arritt, and R. C. Dugan, "The IEEE 8500-Node Test Feeder," in *proc. IEEE PES Transmission & Distribution Conference and Exposition*, 2010.

[25] K. P. Schneider, J. C. Fuller, and D. P. Chassin, "Multi-State Load Models for Distribution System Analysis," *IEEE Trans. on Power Systems*, vol. 26, no. 4. pp. 2425-2433, May 2011.

[26] J. A. Martinez-Velasco, "Transient Analysis of Power Systems: Solution Techniques, Tools and Applications," Wiley, 2015.

[27] H. Lin, S. S. Veda, S. S. Shukla, L. Mili and J. Thorp, "GECO: Global Event-Driven Co-Simulation Framework for Interconnected Power System and Communication Network," *IEEE Trans. on Smart Grid*," vol. 3, no. 3, pp. 1444-1456, May 2012.

[28] T. Hansen, R. Kadavil, B. Palmintier, S. Suryanarayanan, A. Maciejewski, H. Siegel, E. Ching, and E. Hale, :Enabeling Smart Grid Cosimulation Studies: Rapid Design and Development of the Technologies and Controls," IEEE Electrification Magazine, vo. 4, no. 1, pp. 25-32, Feb. 2016.

[29] H. Georg, S. Muller, C. Rehtanz, and C. Wietfeld, "Analyzing Cyber-Physical Energy Systems: The INSPIRE Cosimulation of Power and ICT Systems Using HLA," *IEEE Trans. on Industrial Informatics*, vol. 10, no. 4, pp. 2364-2373, June 2014.

[30] W. H. Kersting, "Distribution System Modeling and Analysis, 3rd Edition," CRC Press, New York, 2012.

[31] P. Irminger *et al*., "Air Conditioning Stall Phenomena - Testing, model Development, and Simulation," in *proc. IEEE PES Transmission & Distribution Conference and Exposition*, 2012.

[32] IEEE Task Force on Load Representation for Dynamic Performance, "Load Representation for Dynamic Performance Analysis," *IEEE Trans. on Power Systems*, vol. 8, no. 2, pp.472-482, May 1993.

[33] IEEE Task Force on Load Representation for Dynamic Performance, "Standard Load Models for Power-flow and Dynamic Performance Simulation," *IEEE Trans. on Power Systems*, vol. 10, no. 3, pp.1302-1313, Aug. 1995.

[34] K. P. Schneider, E. Sortomme, M. T. Miller, S. S. Venkata, and L. Ponder, "Evaluating the Magnitude and Duration of Cold Load Pick-up using Multi-State Load Models," *IEEE Trans. on Power Systems*, vol. 31, no. 5, pp. 3765-3774, Nov. 2016.

[35] B. Lesieutre, D. Kosterev, and J. Undrill, "Phasor Modeling Approach for Single-phase A/C Motors," in *proc. IEEE Power and Energy Society General Meeting*, 2008.

[36] "IEEE Guide for the Presentation of Thermal Limit Curves for Squirrel Cage Induction Machines," *IEEE Std. 620-1996*, pp. 1-12, 1996.

[37] D. Sullivan *et al*., "Managing Fault-Induced Delayed Voltage Recovery in Metro Atlanta with the Barrow County SVC," in *proc. IEEE PES Power Systems Conference and Exposition*, 2009.

[38] K. G. Ravikumar, S. Manson, J. Undrill and J. H. Eto, "Analysis of Fault-Induced Delayed Voltage Recovery using EMTP Simulations," in *proc. IEEE PES Transmission & Distribution Conference and Exposition*, 2016.

[39] L. Pereira , D. N. Kosterev, P. Mackin, D. Davies, J. Undrill, and W. Zhu, "An Interim Dynamic Induction Motor Model for Stability Studies in WSCC," *IEEE Trans. on Power Systems*, vol. 17, no.4, pp. 1108-1115, July 2002.

[40] D. N. Kosterev, et al. "Load Modeling in Power System Studies: WECC Progress Update," in *Proc. IEEE PES General Meeting*, 2008.

[41] North American Electric Reliability Corporation Technical Reference Document, "Dynamic Load Modeling," Tech Reference Document, December 2016.

[42] Q. Huang and V. Vittal, "Application of Electromagnetic Transient-Transient Stability Hybrid Simulation to FIDVR Study," *IEEE Trans. on Power Systems*, vol. 31, no. 4, pp. 2634-2646, Sept. 2016.

[43] R. Bravo and D. Chassin, "Fault Induced Delayed Voltage Recovery (FIDVR) Model Validation," in *Proc. IEEE PES Transmission & Distribution Conference and Exposition*, 2016.

[44] K. P. Schneider, B. A. Mather, B. C. Pal, C. W. Ten, G. J. Shirek, H. Zhu, J. C. Fuller, J. L. R. Pereira, L. F. Ochoa, L. R. de Araujo, R. C. Dugan, S. Matthias, S. Paudyal, T. E. McDermott, and W. Kersting, "Analytic Considerations and Design Basis for the IEEE Distribution Test Feeders," *IEEE Trans. on Power Systems*, vol. PP, no. 99, pp. 1-1, 2017.

[45] D. P. Chassin, K. P. Schneider, and C. Gerkensmeyer, "GridLAB-D: AN Open-Source Power System Modeling and Simulation Environment," in *proc. IEEE PES Transmission and Distribution Conference and Exposition*, 2008.

[46] Typical Meteorological Year Data 2, information available: http://rredc.nrel.gov/solar/old_data/nsrdb/1961-1990/tmy2/ [Accessed: December-2017]

[47] S. E. Zocholl, "Motor Analysis and Thermal Protection," *IEEE Trans. on Power Delivery*, vol. 5, no. 3, pp, 1275-1280, July 1990.

VII. BIOGRAPHIES

Kevin P. Schneider (S'00, M'06, SM'08) received his B.S. degree in Physics and his M.S. and Ph.D. degrees in Electrical Engineering from the University of Washington. His main areas of research are distribution system analysis and power system operations. He is currently a principal research engineer at the Pacific Northwest National Laboratory, working at the Battelle Seattle Research Center in Seattle Washington. Dr. Schneider is an Adjunct Faculty member at Washington State University, an Affiliate Associate Professor at the University of Washington, and is a licensed Professional Engineer in Washington State. He is the past chair of the Distribution System Analysis

Sub-Committee and the current Vice-Chair of the Analytics Methods for Power Systems Committee (AMPS).

Francis Tuffner (S'03, M08) graduated from the University of Wyoming with his PhD in electrical engineering in 2008. He is currently a senior research engineer at the Pacific Northwest National Laboratory. His research interests include signal processing applied to power systems, PHEV integration, embedded control devices, distribution level modeling, and digital signal processing.

Marcelo Elizondo (S'98, M'07, SM'17) completed his Ph.D. in power system engineering at Universidad Nacional de San Juan, Argentina, in 2008. From 2003 to 2005, he was a graduate visiting scholar at Carnegie Mellon University, USA, and he was an undergraduate visitor at Spelec, France in 2001. He worked in Mercados Energ´eticos Consultores (Argentina) from 2007 to 2009, an international power system consulting firm. In 2009 he joined the Pacific Northwest National Laboratory where he is currently a senior research engineer working at the Battelle Seattle Research Center in Seattle Washington. Marcelo's research interests include power system dynamic modeling and control, microgrids, demand response, and HVDC systems.

Jacob Hansen (M'15) received his B.S and M.S degree in electronic engineering and IT from Aalborg University, Denmark in 2012 and 2014, respectively. From September 2013 to May 2014 he was a visiting student with the Active-adaptive Control Laboratory at Massachusetts Institute of Technology. He is currently a research engineer at the Pacific Northwest National Laboratory, working at the Battelle Seattle Research Center in Seattle, Washington. His research interests include power systems, control systems, and Market design. Mr. Hansen was a recipient of the GN Store Nord–Denmark-America Foundation Fellowship in 2013.

Jason Fuller (S'08, M'10, SM'16) received his B.S. degree in physics from the University of Washington and M.S.E.E. from Washington State University. He joined the staff at Pacific Northwest National Laboratory (PNNL) in 2009. He is an active member in IEEE, Vice-Chair of the Distribution System Analysis Subcommittee and Chair of the Test Feeder Working Group. Mr. Fuller's area of interest includes distribution automation and analysis, and integration of advanced distribution-level technologies such as distributed generation and demand response. His main area of work has been in the development and application of GridLAB-D, a power-flow simulation environment designed for smart grid applications and developed at PNNL.

David P. Chassin (M'03, SM'05) received his BS of Building Science from Rensselaer Polytechnic Institute in Troy, New York and his MASc and Ph.D. in Mechanical Engineering from the University of Victoria in Victoria, British Columbia. He is currently a staff scientist in the Grid Integration and Mobility (GISMo) group at SLAC National Accelerator Laboratory in Menlo Park, California. Before joining SLAC, he was a staff scientist at Pacific Northwest National Laboratory (PNNL) where he worked since 1992, leading the development of building energy modeling, control and diagnostic systems, transactive control retail real-time pricing systems, and GridLAB-D™, an open source smart grid simulation built by PNNL for the US Department of Energy. He contributes to the WECC Load Modeling Task Force development of the composite load model. His current research focuses on composite load modeling, control and dispatch of fast-acting demand response, retail real-time demand dispatch using prices, and transactive control theory.